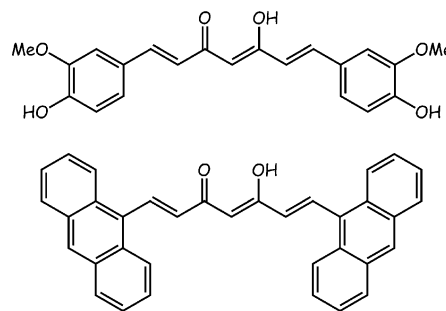


# Dy<sup>III</sup>- and Yb<sup>III</sup>-Curcuminoid Compounds: Original Fluorescent Single-Ion Magnet and Magnetic Near-IR Luminescent Species

Melita Menelaou,<sup>[b]</sup> Fatiha Ouharrrou,<sup>[b]</sup> Laura Rodríguez,<sup>[b]</sup> Olivier Roubeau,<sup>[c]</sup> Simon J. Teat,<sup>[d]</sup> and Núria Aliaga-Alcalde<sup>\*[a]</sup>

The achievement of systems with unique tailor-made properties is the primary target in fields as nanotechnology, nanoelectronics or chemical/biological sensing.<sup>[1]</sup> The breakthrough of “bottom up” methods directly associates with the development of molecules with specific traits, provided with advanced features that will be applicable in favor of faster, more affordable and convenient technologies.<sup>[2]</sup> A coordination chemistry approach uses the synergy between metallic centers and well-thought-out organic arrays that may lead to stable and multifunctional molecular systems. Among the extensive library of organic binders that can be attached to metallic centers, curcuminoid systems (CCMoids) rise as very attractive molecules. The family of CCMoids includes natural and synthetic organic species structurally related to curcumin, CCM (Scheme 1, top).<sup>[3]</sup> In general, they are described as diarylheptanoid chains with central  $\beta$ -diketone moieties and aromatic groups binding both extremes of the chains.<sup>[3]</sup> Even though CCM/CCMoids are extensively studied because of their biomedical applications,<sup>[4]</sup> they are being successfully introduced in other research subjects, including molecular logics.<sup>[5]</sup>

Lately, our research group has gained great deal of experience working with this family of molecules and in particular with a CCMoid called 9Accm, 1,7-di-9-anthracene-1,6-heptadiene-3,5-dione.<sup>[6]</sup> This organic ligand maintains the general traits expected for a CCMoid but with anthracene



Scheme 1. Drawings of curcumin (top) and 9Accm (bottom).

groups in the sides of the conjugated chain (Scheme 1, bottom). Initial research focused on the in vitro activity of the free and coordinated ligand 9Accm with Cu<sup>II</sup>,<sup>[6]</sup> and more recently, on the fluorescence and deposition of a Zn<sup>II</sup>-CCMoid system.<sup>[7]</sup> Also, an innovative method toward the fabrication of gateable room temperature molecular junctions has been tested using free 9Accm as a nanowire capable of anchoring and communicating two graphite surfaces (nanoelectrodes).<sup>[8]</sup> The inherent properties of this molecule (chelating ligand, fluorescent material, easy  $\pi$ - $\pi$  interacting system capable of electronic transport at the nanoscale level) makes it the perfect candidate for the creation of coordination compounds where the attachment of appropriate metallic centers will introduce additional features as well.

From the perspective of the metal, lanthanide-based materials have attracted great interest owing to their unique architectures and potential applications spanning from molecular based magnets and superconductors to light emitting devices and luminescent probes.<sup>[9]</sup> In particular, a limited but promising family of mononuclear Ln<sup>III</sup> species acts as single-ion magnets (SIMs).<sup>[10]</sup> SIMs display slow magnetic relaxation in the absence of dc fields (similar to single-molecular magnets, SMMs), where now the magnetic features are led by the single-ion anisotropy of the Ln under study when it is submitted to a ligand-field (LF).<sup>[10–12]</sup> Great expectations are risen since their discovery owing to the possibility of high anisotropy barriers with several works carried on such characteristic as well as on additional treats, like prominent quantum effects and strong response to internal and external magnetic fields.<sup>[10–12]</sup> Besides, Ln<sup>III</sup> ions can emit either in the UV or in the NIR region depending on their nature and coordination environment.<sup>[9a,b,13]</sup>

[a] Dr. N. Aliaga-Alcalde  
ICREA Researcher  
(Institució Catalana de Recerca i Estudis Avançats)  
at the Universitat de Barcelona, Facultat de Química  
Diagonal 645, 08028 Barcelona (Spain)  
Fax: (+34) 934907725  
E-mail: nuria.aliaga@icrea.cat

[b] Dr. M. Menelaou, F. Ouharrrou, Dr. L. Rodríguez  
Universitat de Barcelona, Facultat de Química  
Diagonal 645, 08028 Barcelona (Spain)

[c] Dr. O. Roubeau  
Instituto de Ciencia de Materiales de Aragón (ICMA)  
CSIC and Universidad de Zaragoza  
Plaza San Francisco s/n 50009 Zaragoza (Spain)

[d] Dr. S. J. Teat  
Advanced Light Source  
Lawrence Berkeley National Laboratory Berkeley  
California 94720 (USA)

Supporting information for this article is available on the WWW under <http://dx.doi.org/10.1002/chem.201200955>.

Our approach involves the specific combination of the aforementioned molecule, 9Accm and Ln metals, to achieve magnetic/luminescent compounds with affinity for graphite surfaces. Herein, we introduce the synthesis and characterization of two Ln-CCMoid compounds: **1**, [Dy(9Accm)<sub>2</sub>(NO<sub>3</sub>)(dmf)<sub>2</sub>] and **2**, [Yb(9Accm)<sub>3</sub>(py)], respectively, analyzed by X-ray diffraction, SQUID magnetic measurements and luminescent spectroscopy. Preliminary data on their deposition on graphite surfaces are described as well.

Both compounds are obtained similarly (see the Supporting Information) by precipitation in dimethylformamide (DMF), although poorer solubility/faster precipitation was observed systematically for the Yb<sup>III</sup> compound. Small but suitable crystals were obtained for **1**·0.75DMF after several days in the concentrated mother liquid; while needle crystals of **2**·py·MeOH were isolated by layering with MeOH a pyridinic solution of the precipitate. Owing to the crystals size and shape, diffraction data for both compounds were collected from synchrotron radiation sources (Table S1 in the Supporting Information depicts the most relevant distances and angles for **1** and **2**).

Compound **1**·0.75DMF crystallizes in the monoclinic space group *P*<sub>n</sub>. A perspective view of the molecular structure is shown in Figure 1A. Each molecule of **1** contains an eight-coordinated Dy<sup>III</sup> ion bounded to two 9Accm ligands, one chelating nitrate group, and two DMF molecules. Dy–O distances are in the range of 2.260–2.540 Å, being the lon-

gest related to one of the Dy–O<sub>NO3</sub> distances. Values of 70.85 and 74.09° were found for the two O<sub>9Accm</sub>–Dy–O<sub>9Accm</sub> angles while a value of 50.87° was obtained for the O<sub>NO3</sub>–Dy–O<sub>NO3</sub> angle. The shortest Dy···Dy distance is 9.283 Å. Overall, compound **1** displays an ideal *D*<sub>2d</sub> symmetry around the Dy atom in which the two 9Accm ligands would be equivalent and the nitrate group together with the two DMF molecules contained in the same plane. Compound **2**·py·MeOH crystallizes in the monoclinic space group *P*<sub>2<sub>1</sub>/c. The total coordination of the Yb<sup>III</sup> ion is now seven as a result of the binding with three 9Accm ligands and a molecule of pyridine (Figure 1B). Extra molecules of pyridine and MeOH participate in the outer sphere (Figure S1 in the Supporting Information). Yb–O<sub>9Accm</sub> distances are between 2.222 and 2.281 Å with a value of 2.523 Å for the Yb–N distance. Angles O<sub>9Accm</sub>–Yb–O<sub>9Accm</sub> are in the range of 75.20–77.38°, similar to those found for **1**. The odd coordination number provides a highly distorted surrounding for the Yb<sup>III</sup> ion, better described as a trigonal prism with a face (Figure S2 in the Supporting Information). Each [Yb(9Accm)<sub>3</sub>(py)] complex remains well isolated from its neighbors; the anthracene groups of the 9Accm ligands protects almost completely the lanthanide ions, where the shortest Yb···Yb distance has a value of 9.835 Å. These structures are the first reported for 4f compounds of CCMoids, those with transition metal ions being also limited to one Ru<sup>III</sup>-CCM,<sup>[14]</sup> two Cu<sup>II</sup>-9Accm and one Zn<sup>II</sup>-9Accm compounds, the last three prepared by us.<sup>[6,7]</sup></sub>

Magnetic studies were performed for **1** and **2** and the temperature dependence of their magnetic properties are shown as  $\chi_m T$  versus *T* in Figure S3 and S4 in the Supporting Information, respectively. The values of  $\chi_m T$  were found to be 14.23 and 2.95 cm<sup>3</sup>mol<sup>−1</sup>K at 300 K for the Dy<sup>III</sup> (*S*=5/2) and the Yb<sup>III</sup> (*S*=1/2) compounds, in that order, in good agreement with expected values (14.17 cm<sup>3</sup>mol<sup>−1</sup>K for a free Dy<sup>III</sup> ion with *J*=15/2, *g*=4/3 and 2.57 cm<sup>3</sup>mol<sup>−1</sup>K for a free Yb<sup>III</sup> ion with a *J*=7/2, *g*=8/7).<sup>[15,16]</sup> Upon cooling, the  $\chi_m T$  value for the two compounds decreases gradually, down to respectively 9.94 and 1.33 cm<sup>3</sup>mol<sup>−1</sup>K at 2 K, which is mostly due to crystal-field effects (thermal depopulation of the Ln<sup>III</sup> Stark sublevels).<sup>[15]</sup> Magnetization versus dc field at 2 K for the two compounds (inset in Figure S3 and S4 in the Supporting Information) are also in agreement with magnetically isolated Dy<sup>III</sup> and Yb<sup>III</sup> ions.

Studies of the magnetization dynamics showed that compound **1** exhibits slow magnetization relaxation. Figure 2 (left) shows the zero-field alternating-current (ac) susceptibility of **1** at various frequencies from 12 to 1.8 K. The out of phase ( $\chi''_m$ ) susceptibilities of compound **1** show strong frequency dependence although no maximum was reached at 1.8 K. However, applying a small applied dc field (0.1 T, right) allows observing peaks in  $\chi''_m$  versus *T*, plots between 2 and 6 K. The characteristic relaxation time  $\tau$  derived from these latter data (using the optimal dc field of 0.1 T) were fit to the Arrhenius relation ( $\tau(T) = \tau_0(U_{\text{eff}}/k_B T)$ ) resulting in a barrier height ( $U_{\text{eff}}/k_B$ ) of 23 K with  $\tau_0 = 1.3 \times 10^{-6}$  s (Figure S5 in the Supporting Information).<sup>[17]</sup> The extrapolation

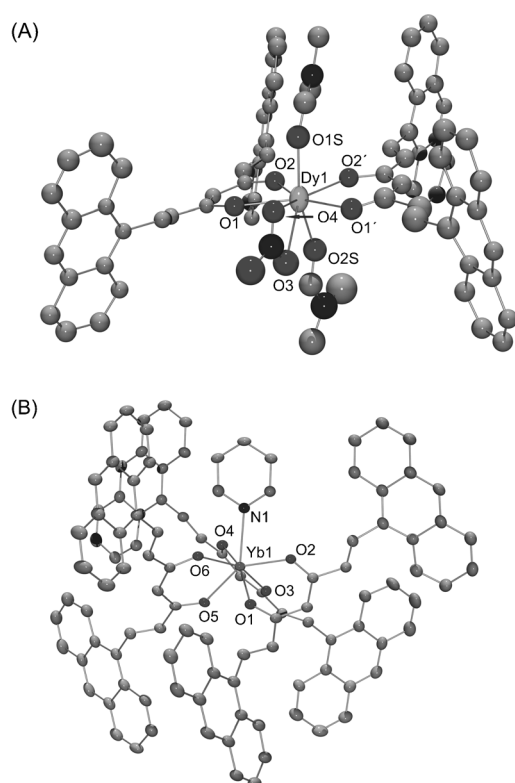


Figure 1. Coordination diagrams and central atoms numbering schemes of A) **1** and B) **2**. Both representations are shown at the 25% ellipsoid probability.

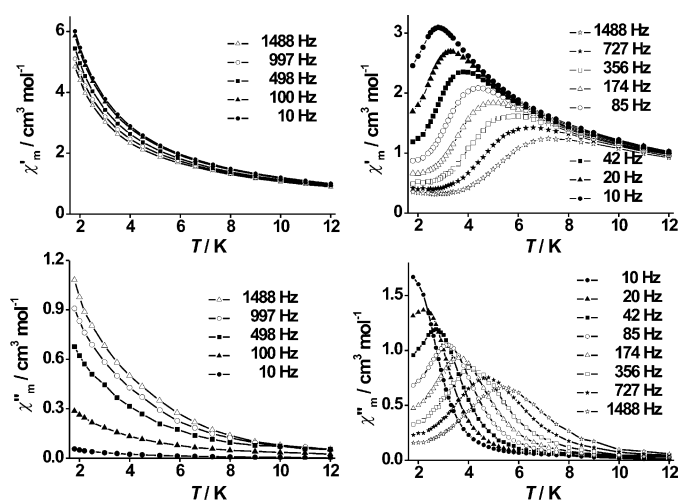


Figure 2. In-phase (top) and out-of-phase susceptibilities of **1** at different frequencies (from 10 to 1488 Hz) at zero applied field (left) and 0.1 T (right).

of the data to zero dc field<sup>[18]</sup> provided a value of  $U_{\text{eff}}/k_B$  close to 15 K (Figure S5 in the Supporting Information). As indicated structurally, the bulky nature of 9Accm ligands ensures good separation among Dy<sup>III</sup> ions and therefore the single-molecule nature of the slow relaxation process of **1**. Cole–Cole diagrams (Figure S6 in the Supporting Information) in the form of  $\chi'_m$  versus  $\chi''_m$  show nearly semi-circular shapes, and have been fit to the generalized Debye model,<sup>[10c,19]</sup> where the  $\alpha$  coefficient shows values in the range of 0.3–0.4 (between 3.0–4.5 K), thus indicating that the tunneling mechanism may be susceptible to local strain.<sup>[19b,c]</sup> These results are in the range of previously reported SMMs and SCMs and excludes the possibility of spin glass.

Among other relevant aspects, the relationship between the Ligand Field geometry around octacoordinated mononuclear Dy<sup>III</sup> species and their single-ion magnet behavior has been highlighted.<sup>[10e]</sup> Related to this matter, we analyzed the geometries for a number of Dy<sup>III</sup> species from the literature using SHAPE v2.0 (Continuous Shape Measures Calculation Program).<sup>[20]</sup> Using this method, it was observed that the most common polyhedron is the square antiprism ( $D_{4d}$ ).<sup>[21]</sup> However, the structural comparison among SIM Dy<sup>III</sup> species (four including compound **1**) shows that three of them display  $D_{4d}$  geometry<sup>[10a,b]</sup> (**1** appears as a distorted square antiprism) and only one is better described using a  $D_{2d}$  polyhedron<sup>[10c]</sup> (Table lists S2 and S3 in the Supporting Information). At this point, the results do not support one geometry over the other (being both indicative of SIM behavior) but rise the big question about the potential magnetic behavior of most of eight-coordinated mononuclear Dy<sup>III</sup> compounds not yet analyzed. It should be also mentioned that additional factors (from ligand-field theory), apart from the shape, are involved in the final magnetic behavior of the systems.<sup>[22,10b]</sup>

In solution, the electronic absorption spectra of the two systems, **1** and **2**, were recorded in THF (concentrations  $10^{-5}$  M); the results are summarized in Table S4 and Figure S7 in the Supporting Information. Both compounds display a very similar behavior presenting an absorption band around 260 nm (assigned to  $\pi \rightarrow \pi^*$  transitions<sup>[23]</sup>), a well-resolved vibrational band in the range of 340–385 nm (related to the anthracene groups), and a third band at approximately 435 nm (typically found in curcumin and derivatives).<sup>[7]</sup> The latter presents slight red shifts compared with the free 9Accm that may be attributed to small differences in the  $\pi$ -electron conjugation upon coordination.<sup>[24]</sup> Similar variations have been observed in analogous 3d compounds with 9Accm, accompanied by changes in color in the final solids, from bright red (free 9Accm) to orange (**1** and **2**).<sup>[6,7]</sup>

Electronic extinction coefficients are the double (for **1**) and the triple (**2**) of that recorded for free 9Accm, agreeing with the number of coordinated 9Accm ligands.<sup>[7]</sup> Upon excitation at 365 or 435 nm, **1–2** present a broad emission band centered at 577 and 578 nm, respectively, with almost identical intensity, (Figure 3) that was associated to 9Accm.

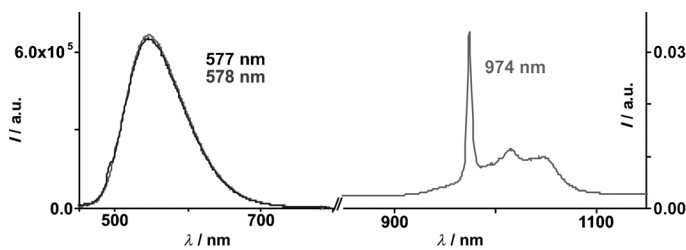


Figure 3. Emission spectra of compound **1** (black line) and **2** (gray line) in  $1 \times 10^{-5}$  M THF solutions ( $\lambda_{\text{exc}} = 435$  nm) in the UV/Vis region (left) and NIR-region (right).

This is similar to the emission band observed for the free ligand but slightly shifted to the red.<sup>[7]</sup> On the other hand, at the same excitation wavelengths, compound **2** exhibits an additional luminescence emission in the near-infrared region with a narrow signal at 974 nm that corresponds to the  $^2F_{5/2} \rightarrow ^2F_{7/2}$  electronic transition. This band is accompanied by broad and weaker bands of lower energy already observed in Yb<sup>III</sup> chelate compounds.<sup>[25,26]</sup> We should note the importance of solvent for the NIR-emission spectrum since similar experiments recorded in  $\text{CH}_2\text{Cl}_2$  only show the emission of Yb at low temperature (very low intensity was observed at room temperature, see Figure S8 in the Supporting Information). Therefore, deactivation mechanisms are favored in  $\text{CH}_2\text{Cl}_2$  in comparison with THF and they are prevented at 77 K. The spectrum of **2** resembles well a related Yb<sup>III</sup> system described by Seltzer et al.<sup>[26]</sup> Previous works have implied the use of CCMoids as sensitizers in a number of reactions and also shown that the triplet state energy expected for CCM and related species is approximately  $14000 \text{ cm}^{-1}$ . On the other hand, it is well known that the principal emitting level of the Yb<sup>III</sup> ion ( $^2F_{5/2}$ ) is in the range of  $10500 \text{ cm}^{-1}$ .<sup>[27]</sup> Thus, it is reasonable to expect a favorable

intramolecular energy transfer from 9Accm to the Yb<sup>III</sup> center.<sup>[28]</sup>

AFM experiments were performed with deposits of **1** and **2** on highly oriented pyrolytic graphite (HOPG) surfaces. The interest on these studies resides in the potential application of this type of support in the construction of nanodevices.<sup>[8]</sup> It has been proved that the anthracene groups of 9Accm easily provide  $\pi$ - $\pi$  interactions with the substrate using simple techniques at room temperature.<sup>[7,8]</sup> Here, spin-coating experiments were performed using dilute solutions of **1** and **2** in CH<sub>2</sub>Cl<sub>2</sub> resulting in evident arrays in both cases (Figure S9B and S9C for **1**; and 4A and S10 for **2**).

At the lowest concentration, AFM images show roughly homogeneous heights, with values between 0.6 nm and 1.3 nm for **1** and **2** (Figure S11 in the Supporting Information). The values are smaller than the ones found by strict comparison with their molecular structures (e.g., highest distances of about 1.6 nm for **2**). This could be explained by the interaction of anthracene groups with the graphite surface and therefore, rearrangement of these anthracene moieties with respect to their attached diarylheptanoid chains; also changes in the conformations of the double bonds of the same chains (*Z/E* isomerism) may provide folding effects decreasing the total height. Figure S12 in the Supporting Information shows some examples of distances for **2** taking into account such considerations. Based on both statements, distances agree well with the ones found by AFM (e.g., between 0.65 and 0.95 nm for **2**). In addition, more concentrated solutions of **2** (10<sup>-4</sup> M) provided multilayer aggregates (Figure 4B). AFM images heights were now

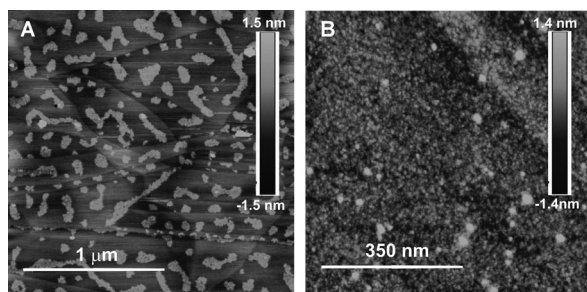


Figure 4. AFM images of HOPG surfaces after adding A) a solution 10<sup>-5</sup> M of **2** in CH<sub>2</sub>Cl<sub>2</sub> and B) a solution 10<sup>-4</sup> M of **2** in CH<sub>2</sub>Cl<sub>2</sub>.

between 2.0 and 2.7 nm (Figure S13 in the Supporting Information), that compared with the lowest concentration suggest the formation of approximately 3–5 layers of stacked molecules. This fact was also observed in the past for similar molecules.<sup>[8]</sup> These experiments evidence interactions between molecules of **1** and **2**, and HOPG. Molecular disposition relates to molecule–surface interactions but also to additional parameters such as applied methods, supramolecular interactions among molecules and therefore concentration.<sup>[6,7]</sup> Nevertheless, further studies using STM will follow to fully discuss such factors; STM-electroluminescence will also be of great interest due to the number of chromo-

phores, making compounds **1** and **2** promising as potential fluorescent systems at the nanoscale level.<sup>[29]</sup>

In summary, this work reports the first two crystallographically characterized 4f compounds with CCMoid ligands. The Dy<sup>III</sup> compound (**1**) presents single-ion magnet properties and constitutes a new addition to the still limited family of mononuclear Ln systems that exhibit SIM behavior. Moreover, **1** displays luminescence in the visible region showing a broad emission band at 577 nm (due to the fluorescent nature of 9Accm). In that respect, the Yb<sup>III</sup> compound (**2**) exhibits two emission bands, one similar to **1** in the visible, and another in the near-infrared region at 974 nm. Both systems have been successfully deposited on graphite surfaces.

## Experimental Section

Starting materials were purchased from Aldrich and all manipulations were performed using materials as received. Ligand 9Accm was synthesized as reported elsewhere.<sup>[1]</sup>

**Preparation of [Dy(9Accm)<sub>2</sub>(NO<sub>3</sub>)(dmf)<sub>2</sub>] (**1**):** Dy(NO<sub>3</sub>)<sub>3</sub>·6H<sub>2</sub>O (191.0 mg, 0.4 mmol) was dissolved in dimethylformamide (DMF, 20 mL) while 9Accm (200 mg, 0.4 mmol) was dissolved in DMF (35 mL) and deprotonated with 0.8 mL of an aqueous solution of KOH (22.0 mg, 0.4 mmol). Following that, the ligand solution was added dropwise under continuous stirring to the metal solution, resulting in a rapid color change to orange. The reaction mixture was stirred for two days and the final volume decreased to nearly 5 mL under reduced pressure. After several days, an orange crystalline solid appeared. The dry solid was washed with water, methanol, and ether and dried in air. Yield: 55%; IR (KBr):  $\tilde{\nu}$  = 1651 (s), 1564 (w), 1508 (s), 1427 (s), 1384 (w), 1307 (w), 1156 (w), 973 (w), 885 (w), 735 cm<sup>-1</sup> (m); MS (ESI): *m/z* (%): 1141 [*M*]<sup>+</sup>; elemental analysis calcd (%) for 1·0.75DMF (C<sub>76</sub>H<sub>54</sub>DyN<sub>3</sub>O<sub>9</sub>): C 70.53, H 4.20, N 1.99; found: C 70.82, H 4.49, N 1.91.

**Preparation of [Yb(9Accm)<sub>3</sub>(py)] (**2**):** Yb(NO<sub>3</sub>)<sub>3</sub>·6H<sub>2</sub>O (188.5 mg, 0.4 mmol) was dissolved in dimethylformamide (DMF, 20 mL) while 9Accm (200.0 mg, 0.4 mmol) was dissolved in DMF (35 mL) and deprotonated with 0.8 mL of an aqueous solution of KOH (22.0 mg, 0.4 mmol). In addition, the ligand solution was added dropwise under continuous stirring to the metal solution, resulting in a rapid color change to orange. The reaction mixture was stirred until an orange solid resulted after several hours. The powder was washed several times with water, methanol, and diethyl ether and dissolved in pyridine. Finally, crystals of **2** were achieved from layering of the solution with MeOH. Yield: 40%; IR (KBr):  $\tilde{\nu}$  = 1661 (m), 1630 (m), 1550 (m), 1508 (s), 1418 (s), 1353 (w), 1157 (m), 999 (w), 976 (w), 881 (w), 732 cm<sup>-1</sup> (m); MS (ESI): *m/z* (%): 1124.3 [*M*]<sup>+</sup>, 649.1 [*M*+MeCN]<sup>+</sup>; elemental analysis calcd for 2·1.5DMF·0.5 MeOH (C<sub>116</sub>H<sub>83</sub>YbN<sub>2</sub>O<sub>7</sub>): C 76.57, H 4.76, N 1.22; found: C 76.44, H 4.66, N 1.25.

CCDC-870041 (**2**) and CCDC-870042 (**1**) contain the supplementary crystallographic data for this paper. These data can be obtained free of charge from The Cambridge Crystallographic Data Centre via [www.ccdc.cam.ac.uk/data\\_request/cif](http://www.ccdc.cam.ac.uk/data_request/cif).

## Acknowledgements

We thank the MICINN (CTQ2009-06959/BQU and CTQ2009-08795) for financial support. The Advanced Light Source is supported by the Director, Office of Science, Office of Basic Energy Sciences, of the U.S Department of Energy under Contract No. DE-AC02-05CH11231. N.A.-A. thanks Prof. Eliseo Ruiz, Dr. Núria Clos, and Dr. Gerard Oncins from the UB.

**Keywords:** curcuminoid • lanthanides • luminescence • magnetic properties • X-ray diffraction

- [1] A. Coskun, M. Banaszak, R. D. Astumian, J. F. Stoddart, B. A. Grzybowski, *Chem. Soc. Rev.* **2012**, *41*, 19–30.
- [2] R. Mas-Ballesté, J. Gómez-Herrero, F. Zamora, *Chem. Soc. Rev.* **2010**, *39*, 4220–4233.
- [3] L. J. Bellamy, G. S. Spicer, J. D. H. Strickland, *J. Chem. Soc.* **1952**, *74*, 4653–4656.
- [4] E. Nakta, M. Koizumi, Y. Yamshita, K. Onaka, Y. Sakurai, N. Kondo, K. Ono, Y. Uto, H. Horii, *Anticancer Res.* **2011**, *31*, 2477–2482.
- [5] S.-H. Kim, S.-Y. Gwon, S. M. Burkinshaw, Y.-A. Son, *Spectrochim. Acta Part A* **2010**, *76*, 384–387.
- [6] N. Aliaga-Alcalde, P. Marqués-Gallego, M. Kraaijkamp, C. Herranz-Lancho, H. den Dulk, H. Görner, O. Roubeau, S. J. Teat, T. Weyhermüller, J. Reedijk, *Inorg. Chem.* **2010**, *49*, 9655–9663.
- [7] N. Aliaga-Alcalde, L. Rodríguez, M. Ferbinteanu, P. Höfer, T. Weyhermüller, *Inorg. Chem.* **2012**, *51*, 864–873.
- [8] F. Prins, A. Barreiro, J. W. Ruitenberg, J. S. Seldenthuis, N. Aliaga-Alcalde, L. M. K. Vandersypen, H. S. J. van der Zant, *Nano Lett.* **2011**, *11*, 4607–4611.
- [9] A. J. Drew, C. Niedermayer, P. J. Baker, F. L. Pratt, S. J. Blundell, T. Lancaster, R. H. Liu, G. Wu, X. H. Chen, I. Watanabe, V. K. Malik, A. Dubroka, M. Rössle, K. W. Kim, C. Baines, C. Bernhard, *Nat. Mater.* **2009**, *8*, 310–314.
- [10] a) N. Ishikawa, M. Sugita, N. Tanaka, T. Ishikawa, S.-ha. Koshihara, Y. Kaizu, *Inorg. Chem.* **2004**, *43*, 5498–5500; b) M. A. AlDamen, J. M. Clemente-Juan, E. Coronado, C. Martí-Gastaldo, A. Gaita-Ariño, *J. Am. Chem. Soc.* **2008**, *130*, 8874–8875; c) S.-D. Jiang, B.-W. Wang, G. Su, Z.-M. Wang, S. Gao, *Angew. Chem.* **2010**, *122*, 7610–7613; *Angew. Chem. Int. Ed.* **2010**, *49*, 7448–7451; d) D.-P. Li, T.-W. Wang, Li, D.-S. Liu, Y.-Z. Li, X.-Z. You, *Chem. Commun.* **2010**, *46*, 2929–2931; e) G.-J. Chen, C.-Y. Gao, J.-L. Tian, J. Tang, W. Gu, X. Liu, S.-P. Yan, D.-Z. Liao, P. Cheng, *Dalton Trans.* **2011**, *40*, 5579–5583; f) S.-D. Jiang, B.-W. Wang, H.-L. Sun, Z.-M. Wang, S. Gao, *J. Am. Chem. Soc.* **2011**, *133*, 4730–4733.
- [11] J. D. Rinehart, J. R. Long, *Chem. Sci.* **2011**, *2*, 2078–2085.
- [12] a) F. Luis, M. J. Martínez-Pérez, O. Montero, E. Coronado, S. Cardona-Serra, c. Martí-Gastaldo, J. M. Clemente-Juan, J. Sesé, D. Drung, T. Schurig, *Phys. Rev. B* **2010**, *82*, 060403; b) P.-E. Car, M. Perfetti, M. Mannini, A. Favre, A. Caneschi, R. Sessoli, *Chem. Commun.* **2011**, *47*, 3751–3753.
- [13] L. D. Carlos, R. A. S. Ferreira, V. de Zea Bermudez, S. J. L. Ribeiro, *Adv. Mater.* **2009**, *21*, 509–534.
- [14] F. Kühlwein, K. Polborn, W. Z. Beck, *Z. Anorg. Allg. Chem.* **1997**, *623*, 1211–1219.
- [15] L. Di Bari, P. Salvatori, *Coord. Chem. Rev.* **2005**, *249*, 2854–2879.
- [16] O. Kahn, in *Molecular Magnetism*, VCH, Weinheim, **1993**, pp. 47.
- [17] N. Ishii, Y. Okamura, S. Chiba, T. Nogami, T. Ishida, *J. Am. Chem. Soc.* **2008**, *130*, 24–25.
- [18] J. Martínez-Lillo, D. Armentano, G. De Munno, W. Wernsdorfer, J. M. Clemente-Juan, J. Krzystek, F. Lloret, M. Julve, J. Faus, *Inorg. Chem.* **2009**, *48*, 3027–3038.
- [19] a) K. S. Cole, R. H. Cole, *J. Chem. Phys.* **1941**, *9*, 341–351; b) K. Bernot, F. Pointillart, P. Rosa, M. Etienne, R. Sessoli, D. Gatteschi, *Chem. Commun.* **2010**, *46*, 6458–6460; c) Y.-N. Guo, G.-F. Xu, Y. Guo, J. Tang, *Dalton Trans.* **2011**, *40*, 9953–9963.
- [20] D. Casanova, M. Llunell, P. Alemany, S. Alvarez, *Chem. Eur. J.* **2005**, *11*, 1479–1494.
- [21] From a total of 86  $O_h$  mononuclear Dy<sup>III</sup> compounds, 45 were better described using a square antiprism polyhedron ( $D_{4d}$ ), 29 a triangular dodecahedron ( $D_{2d}$ ), 8 as biaugmented trigonal prism ( $C_{2v}$ ) and 4 with a cube shape.
- [22] a) N. Ishikawa, T. Iino, Y. Kaizu, *J. Phys. Chem. A* **2002**, *106*, 9543; b) N. Ishikawa, T. Iino, Y. Kaizu, *J. Am. Chem. Soc.* **2002**, *124*, 11440; c) M. A. AlDamen, S. Cardona-Serra, J. M. Clemente-Juan, E. Coronado, A. Gaita-Ariño, C. Martí-Gastaldo, F. Luis, O. Montero, *Inorg. Chem.* **2009**, *48*, 3467–3479.
- [23] a) K. Krishnakutty, P. Venugopalan, *Synt. React. Inorg. Met.-Org. Chem.* **1998**, *28*, 1313–1325; b) V. D. John, K. Krishnakutty, *Trans. Met. Chem.* **2005**, *30*, 229–233; c) V. D. John, K. Krishnakutty, *Appl. Organomet. Chem.* **2006**, *20*, 477–482.
- [24] a) F. Zsila, Z. Bikadi, M. Simonyi, *Biochem. Biophys. Res. Commun.* **2003**, *301*, 776–782; b) K. I. Priyadarsini, *J. Photochem. Photobiol. C* **2009**, *10*, 81–95.
- [25] W. G. Perkins, G. A. Crosby, *J. Chem. Phys.* **1965**, *42*, 407–411.
- [26] M. D. Seltzer, S. Fallis, R. A. Hollins, N. Prokopuk, R. N. Bui, *J. Fluoresc.* **2005**, *15*, 597–603.
- [27] H. Yersin, K. L. Bray, in *Transition Metal and Rare Earth Compounds: Excited states, transitions, interactions II*, Springer, Berlin, **2001**, p. 51.
- [28] a) G. Zucchi, R. Scopelliti, J.-C. G. Bünzli, *J. Chem. Soc. Dalton Trans.* **2001**, 1975–1985; b) Y. Luo, Q. Yan, S. Wu, W. Wu, Q. Zhang, *J. Photochem. Photobiol. A* **2007**, *191*, 91–96; c) W. Xiaofan, *J. Rare Earths* **2010**, *28*, 246–249.
- [29] a) G. te Velde, F. M. Bickelhaupt, S. J. A. van Gisbergen, C. Fonseca Guerra, E. J. Baerends, J. G. Snijders, T. Ziegler, *J. Comput. Chem.* **2001**, *22*, 931–967; b) C. Fonseca Guerra, J. G. Snijders, G. te Velde, E. J. Baerends, *Theor. Chem. Acc.* **1998**, *99*, 391–403; c) S. Alves, F. Pina, M. T. Albelda, E. García-España, C. Soriano, S. V. Luis, *Eur. J. Inorg. Chem.* **2001**, 405–412; d) S.-H. Kim, S.-Y. Gwon, S. M. Burkinshaw, Y.-A. Son, *Spectrochim. Acta Part A* **2010**, *76*, 384–387.

Received: March 20, 2012

Revised: May 17, 2012

Published online: July 31, 2012